

A cusp electron gun for millimeter wave gyrodevices

C. R. Donaldson,^{a)} W. He, A. W. Cross, F. Li, A. D. R. Phelps, L. Zhang, K. Ronald, C. W. Robertson, C. G. Whyte, and A. R. Young

Department of Physics, SUPA, University of Strathclyde, Glasgow G4 0NG, United Kingdom

(Received 18 January 2010; accepted 8 March 2010; published online 5 April 2010)

The experimental results of a thermionic cusp electron gun, to drive millimeter and submillimeter wave harmonic gyrodevices, are reported in this paper. Using a “smooth” magnetic field reversal formed by two coils this gun generated an annular-shaped, axis-encircling electron beam with 1.5 A current, and an adjustable velocity ratio α of up to 1.56 at a beam voltage of 40 kV. The beam cross-sectional shape and transported beam current were measured by a witness plate technique and Faraday cup, respectively. These measured results were found to be in excellent agreement with the simulated results using the three-dimensional code MAGIC. © 2010 American Institute of Physics. [doi:10.1063/1.3374888]

Further to the design and numerical optimization of a cusp electron beam source,¹ in this paper we present the experiment of the cusp gun and the measured results of the generated axis-encircling electron beam. Due to its small cross-sectional size (less than 1 mm in diameter) in a large magnetic field (a few tesla) such a beam is capable of driving millimeter and submillimeter wave gyrodevices which have many modern applications notably in remote sensing,² medical imaging,³ plasma heating,⁴ and electron spin resonance spectroscopy.⁵ In order to reach higher frequencies, gyrodevices are more commonly operating at a higher indexed waveguide mode and a harmonic of the electron cyclotron frequency;^{6–10} the advantage being that it lowers the required magnetic field strength by a factor of s , the harmonic number. However, operating at harmonics could introduce undesired mode competition, as well as parasitic oscillations. An axis-encircling electron beam is ideal for harmonic gyrodevices due to its good mode selectivity as the beam-wave coupling requires that the azimuthal index of the waveguide mode, m be equal to s .¹¹ Compared to previous cusp guns,^{12–15} this cusp gun has the advantage of (1) simple design and structure with reduced manufacturing complexity due to the “smooth cusp” configuration¹⁶ using two coils without any need for extra magnetic poles and/or material and (2) smaller cusp amplitude because the cusp is located immediately after the cathode where the electron is not fully accelerated.

The electron gun was designed and optimized using the three-dimensional particle-in-cell code MAGIC. The applications were for three microwave sources being developed including a W-band gyrotron backward-wave oscillator (gyro-BWO)¹⁷ and a W-band gyrotron traveling-wave tube¹⁸ both using a helically corrugated waveguide and a terahertz seventh harmonic gyrotron.¹⁹ These devices are based on the previous radiation sources operating at X-band (8.4 to 12 GHz) frequencies.^{20–22} The cusp gun was designed to generate an electron beam of 1.5 A, 40 kV with velocity ratio $\alpha = 1–3$ in order to generate millimeter and submillimeter waves of 75 GHz to 390 GHz over a magnetic field range of 1.50–2.1 T. Based on the simulation results for one particular set of parameters which yields an optimized beam for an

alpha range of 1–2, the cusp electron gun of Fig. 1 was manufactured.

The cathode assembly and the anode were arranged in a coaxial configuration (Fig. 1). The cathode head included three following interchangeable parts: outer, inner focusing electrodes, and the thermionic cathode emitter which was located between the electrodes and constructed from porous tungsten impregnated with barium oxide. Facing the cathode head was an interchangeable anode tip. The beam trajectories are determined by the dimensions of these interchangeable parts. The cathode heating coil was bifilar wound in order to minimize any contribution to the field at the cathode.¹ Two fine gaps of 0.1 mm in width between the emitter and the focusing electrodes were used to reduce the thermal loading of the cathode and to stop the migration of barium from the emitter. Layers of thin tubes and disks made from molybdenum, located between the outer electrodes and the emitter and behind the emitter, respectively, were used as radiation shields to further reduce the thermal loading of the cathode. The beam tunnel tapered down from the anode aperture (radius 4 mm) to the cut-off filter (radius 0.84 mm), followed by an experimental region, a cylindrical tunnel of radius 3.0 mm and length 292 mm, and then to the up-taper and finally the window region. This experimental region allowed the beam diagnostic apparatus such as the Faraday cup and the scintillator witness plate to be inserted. A single layer sapphire window was used in this beam experiment for observation of the visible light generated by the scintillator. The whole system was evacuated to 10^{-9} mBar.

The magnetic field coils were wound from annealed, varnish-coated, square copper wire of cross section 2.2×2.2 mm², enclosed in watertight, stainless steel chambers, and cooled by high pressure recirculating water when in operation. The cavity solenoid which generates a uniform B-field in the beam-wave interaction region has 14 layers each of 103 turns. Two extra layers of coils were added to both ends of the main solenoid to reduce the rise and fall distance of its B-field profile for a certain length of the flat-top so that the overall turns, length of the solenoid, and hence the driving electric power were reduced. At maximum achievable magnetic field strength of 2.1 T the required driving power was ~ 65 kW at a current of ~ 270 A. The layers were separated by 0.4 mm gaps to allow cooling water to

^{a)}Electronic mail: craig.donaldson@strath.ac.uk.

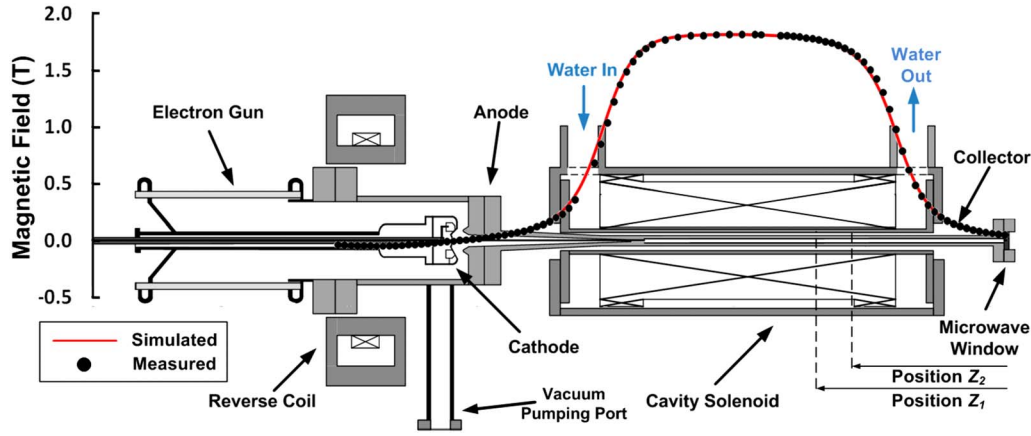


FIG. 1. (Color online) Schematic diagram of the cusp electron gun with simulated and measured magnetic field profile overlaid.

pass from one end to the other end of the solenoid. Simulations of the fluid dynamics and heat exchange including heat conduction, convection, and diffusion were performed by using the MultiPhysics code COMSOL.²³ The reverse coil, having four layers each of ten turns, produced the reverse B-field for the cusp gun. The magnetic field profiles measured using an axial Hall probe and calculated from MAGIC are shown in Fig. 1.

A double cable Blumlein²⁴ which could output a ~ 380 ns, 40 kV pulse was used to drive the cusp gun. The beam voltage was measured using a two-stage voltage divider made from metal film resistors. The emitted current was measured with a Rogowski coil located in the earth line between the anode and the cable Blumlein and the beam current by a Faraday cup at Z_1 location (see Fig. 1).

The beam cross-sectional shape and dimensions were recorded by a phosphor scintillator plate and digital camera system²⁵ after the Faraday cup was removed. The scintillator, a round transparent disk coated with a thin layer of phosphor, produces visible light when electrons impact on the surface. A thin titanium disk of thickness ~ 8 μm was placed before the scintillator to reduce the impact energy of the beam. The scintillator disk was located at position Z_2 (see Fig. 1), 10.5 cm from the window so as to match with the focal length of the camera, at this position the magnetic field tailed off to 90% of the cavity B-field. By using the equation in Ref. 16, the α value in the cavity (in particular, at Z_1) could be calculated from the B-field and α values at Z_2 .

Typical traces of beam voltage and beam current are shown in Fig. 2. The emitted current from the cathode could be varied from 0 to ~ 1.6 A by increasing the operating

temperature of the cathode, at the applied beam voltage of 40 kV. Further increase in the temperature did not result in an increase in the beam current. This indicated that the operation of the cathode had become space-charge limited. In Fig. 2, we can see the beam current reached a steady value of 1.5 A. When the cavity B-field was 1.82 T $\sim 96\%$ of this current reached the Faraday cup.

A typical scintillator image, after the optical noise was removed, is shown in Fig. 3. The image shows clearly that an axis-encircling electron beam was generated. The simulated beam cross-sectional shape is shown for comparison together with beam trajectories in the R - Z plane. For this particular measurement, at a cavity B-field of 1.64 T, the annular beam was measured to have an average radius of ~ 0.37 mm. It was calculated from the equation in Ref. 16 that the corresponding α was 1.34 ± 0.11 . This corresponded to an α value of 1.56 ± 0.16 at the Z_1 position.

By adjusting the reverse coil current the magnetic field at the cathode and hence the value of the velocity ratio of the beam in the cavity could be controlled. At $B_0 = 1.64$ T the velocity ratio at position Z_2 as a function of cathode B-field was measured and is shown in Fig. 4. For comparison of the simulated α at Z_1 and Z_2 as well as analytically calculated value at Z_2 are also shown in Fig. 4. From the diagram, the measured α value had the same trend and good agreement with both the numerical simulated and analytically calculated values. However investigation at higher alphas was limited by the capability of the existing power supply.

In summary, when the thermionic cusp gun for millimeter/submillimeter wave gyrodevices was tested, the

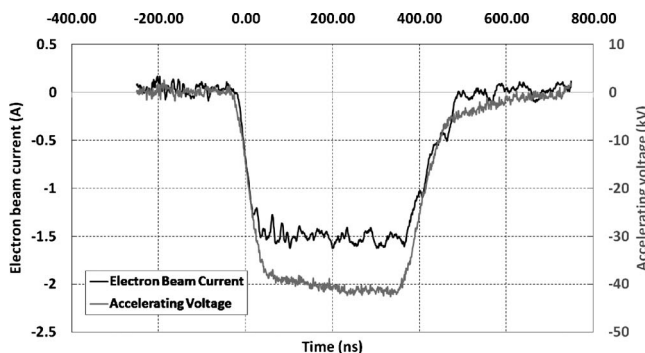


FIG. 2. The typical traces of the measured beam voltage and beam current.

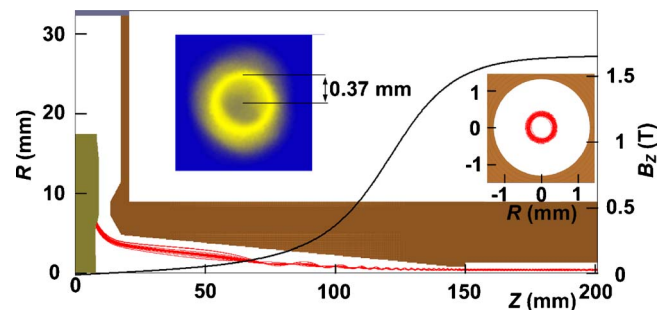


FIG. 3. (Color online) Snapshot of the simulated electron beam trajectory with magnetic field profile overlaid, also simulated and scintillator recorded beam cross-sectional shape at the downstream region.

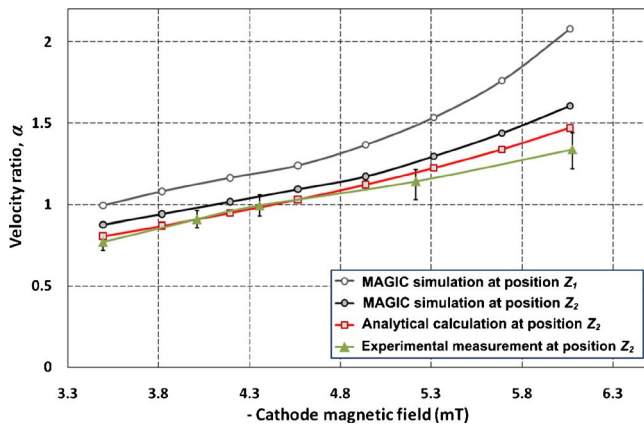


FIG. 4. (Color online) The measured, simulated, and analytically calculated beam velocity ratio as a function of cathode magnetic field at $B_0=1.64$ T.

measured beam parameters were in excellent agreement with the MAGIC simulation. In addition, in a recent experiment, the beam from this cusp gun has been used in a helical waveguide gyro-BWO which generated microwave radiation in the frequency range 92–100 GHz.²⁶

The authors would thank the UK Engineering and Physical Sciences Research Council, the UK Faraday Partnership in High Power RF, the Scottish Universities Physics Alliance and Overseas Research Students Awards Scheme for supporting this work.

¹C. R. Donaldson, W. He, A. W. Cross, A. D. R. Phelps, F. Li, K. Ronald, C. W. Robertson, C. G. Whyte, A. R. Young, and L. Zhang, *IEEE Trans. Plasma Sci.* **37**, 2153 (2009).

²W. M. Manheimer, G. Mesyats, and M. I. Petelin, in *Applications of High-Power Microwaves*, edited by A. V. Gaponov-Grekhov and V. L. Granatstein (Artech House, Norwood, 1994), pp. 169–207.

³R. M. Woodward, B. E. Cole, R. J. Pye, D. D. Amone, E. H. Linfield, and M. Pepper, *Phys. Med. Biol.* **47**, 3853 (2002).

⁴T. Imai, N. Kobayashi, R. Temkin, M. Thumm, M. Q. Tran, and V. Alikaev, *Fusion Eng. Des.* **55**, 281 (2001).

⁵H. M. Assenheim, *Introduction to Electron Spin Resonance* (Plenum, New York, 1966).

⁶M. Garven, J. P. Calame, B. G. Danly, K. T. Nguyen, B. Levush, F. N. Wood, and D. E. Pershing, *IEEE Trans. Plasma Sci.* **30**, 885 (2002).

⁷G. F. Brand, P. W. Fekete, K. Hong, K. J. Moore, and T. Idehara, *Int. J. Electron.* **68**, 1099 (1990).

⁸T. Idehara, I. Ogawa, S. Mitsudo, Y. Iwata, S. Watanabe, Y. Itakura, K. Ohashi, H. Kobayashi, T. Yokoyama, V. E. Zapevalov, M. Y. Glyavin, A. N. Kufin, O. V. Malygin, and S. P. Sabchevski, *IEEE Trans. Plasma Sci.* **32**, 903 (2004).

⁹T. H. Chang, C. F. Yu, C. L. Hung, Y. S. Yeh, M. C. Hsiao, and Y. Y. Shin, *Phys. Plasmas* **15**, 073105 (2008).

¹⁰Q. S. Wang, H. E. Huey, D. B. McDermott, Y. Hirata, and N. C. Luhmann, Jr., *IEEE Trans. Plasma Sci.* **28**, 2232 (2000).

¹¹K. R. Chu, *Rev. Mod. Phys.* **76**, 489 (2004).

¹²J. Sinnis and G. Schmidt, *Phys. Fluids* **6**, 841 (1963).

¹³M. Friedman, *Phys. Rev. Lett.* **24**, 1098 (1970).

¹⁴W. Lawson, *Appl. Phys. Lett.* **50**, 1477 (1987).

¹⁵S. G. Jeon, C. W. Baik, D. H. Kim, G. S. Park, N. Sato, and K. Yokoo, *Appl. Phys. Lett.* **80**, 3703 (2002).

¹⁶W. He, C. G. Whyte, E. G. Rafferty, A. W. Cross, A. D. R. Phelps, K. Ronald, A. R. Young, C. W. Robertson, D. C. Speirs, and D. H. Rowlands, *Appl. Phys. Lett.* **93**, 121501 (2008).

¹⁷C. R. Donaldson, W. He, A. D. R. Phelps, F. Li, A. W. Cross, K. Ronald, A. R. Young, and C. G. Whyte, *Joint 33rd International Conference on Infrared and Millimeter and 16th International Conference on Terahertz Electronics*, Pasadena, CA, 2008 (IEEE, New York, 2008).

¹⁸W. He, A. D. R. Phelps, A. W. Cross, C. R. Donaldson, and K. Ronald, The 17th High-Power Particle Beams Conference (Beams' 08), Xi'an, China (Chinese Pulsed Power Society, Chinese Particle Accelerator Society, 2008), p. 646.

¹⁹F. Li, W. He, A. D. R. Phelps, A. W. Cross, C. R. Donaldson, and K. Ronald, *Joint 33rd International Conference on Infrared and Millimeter and 16th International Conference on Terahertz Electronics*, Pasadena, CA, 2008 (IEEE, New York, 2008).

²⁰A. W. Cross, W. He, A. D. R. Phelps, K. Ronald, C. G. Whyte, A. R. Young, C. W. Robertson, E. G. Rafferty, and J. Thomson, *Appl. Phys. Lett.* **90**, 253501 (2007).

²¹W. He, K. Ronald, A. R. Young, A. W. Cross, A. D. R. Phelps, C. G. Whyte, E. G. Rafferty, J. Thomson, C. W. Robertson, E. C. Speirs, S. V. Samsonov, V. L. Bratman, and G. G. Denisov, *IEEE Trans. Electron Devices* **52**, 839 (2005).

²²W. He, A. W. Cross, A. D. R. Phelps, K. Ronald, C. G. Whyte, S. V. Samsonov, V. L. Bratman, and G. G. Denisov, *Appl. Phys. Lett.* **89**, 091504 (2006).

²³COMSOL, Multiphysics, Comsol, Inc., www.comsol.com

²⁴I. C. Somerville, S. J. MacGregor, and O. Farish, *Meas. Sci. Technol.* **1**, 865 (1990).

²⁵W. He, H. Yin, A. D. R. Phelps, A. W. Cross, and S. N. Spark, *Rev. Sci. Instrum.* **72**, 4266 (2001).

²⁶W. He, C. R. Donaldson, A. W. Cross, F. Li, A. D. R. Phelps, L. Zhang, K. Ronald, C. W. Robertson, C. G. Whyte, and A. R. Young, The 34th International Conference on Infrared, Millimeter, and Terahertz Waves, Busan, Korea (IEEE, New York, 2009).